

SCALAR ELECTRON PRODUCTION IN e^+e^- ANNIHILATION

M. KURODA

Institute of Theoretical Physics, University of Regensburg, Regensburg, Fed. Rep. Germany

K. ISHIKAWA¹

Deutsches Elektron-Synchrotron, DESY, Hamburg, Fed. Rep. Germany

and

T. KOBAYASHI and S. YAMADA

Laboratory of International Collaboration on Elementary Particle Physics, University of Tokyo, Tokyo, Japan

Received 7 April 1983

The single scalar electron production process $e^+e^- \rightarrow e^\pm + \text{photino} + \text{scalar electron}$ (scalar electron $\rightarrow e^\mp + \text{photino}$), with the detection of e^+ as well as e^- , provides a clean method to detect scalar electrons when their masses are not lighter than the beam energy. We made a complete calculation of the process and evaluated the production cross sections.

There is now much interest in supersymmetric theories [1]. In such theories, to each spin 1/2 leptons ℓ , two charged spin 0 leptons are associated, which we denote by s_ℓ and t_ℓ , while to each gauge particle there exists corresponding spinors, e.g., the photino as a supersymmetric partner of the photon. Since no s_e nor t_e with the same mass as that of electron are observed in nature, the symmetry must be apparently broken and is not manifest at low energies, which is at our disposal. It is clearly important to develop a detailed phenomenology in order to test such theories^{†1}.

In this paper, we consider a clean method of hunting for scalar electrons in e^+e^- annihilation. When the beam energy is high enough, the scalar electrons can be pair-produced in e^+e^- annihilation [3]. If the mass of the scalar electron is larger than the beam energy, as it has been shown to be the case by the PETRA experiments [4], they will be produced singly in association with the photino, $\tilde{\gamma}$, the supersymmetric partner of the photon. This possibility,

$e^+e^- \rightarrow e^\pm \tilde{\gamma} t_e^\mp, e^\pm \tilde{\gamma} s_e^\mp$, is studied in ref. [5], in which the Weizsäcker–Williams approximation is used to integrate over the unobserved final e^\pm . In this case, however, there is a problem of large backgrounds, such as coming from $e^+e^- \rightarrow e^+e^- \gamma$, from $e^+e^- \rightarrow \tau^+\tau^-\gamma$ and from two-photon processes, which must be carefully distinguished from the scalar electron production processes.

We propose to study the process $e^+e^- \rightarrow e^\pm \tilde{\gamma} t_e^\mp, e^\pm \tilde{\gamma} s_e^\mp$, with simultaneous detection of e^\pm . This kind of coincidence experiment has, in general, a small cross section but it eliminates almost all possible backgrounds and becomes a very clean experiment for scalar electrons. The events produce a single e^\pm with large transverse momentum and a single scalar electron, with missing photino. The produced scalar electron decays promptly into an e^\mp and a photino, and the final states become e^+e^- plus missing energy^{‡2}.

^{‡2} We assume that the photino does not decay inside the detector. If the gravitino, \tilde{G} , is lighter than the photino, the dominant decay mode of the photino is expected to be $\tilde{\gamma} \rightarrow \gamma \tilde{G}$. The decay width of this mode is extremely model dependent but is expected to be small when \tilde{G} is light. We assume that it is the case and that the photino produced in the process escapes detection.

¹ Present address: Department of Physics, City college of New York, New York, USA.

^{†1} For recent investigations, see ref. [2].

The lagrangian responsible to the reaction is [6],

$$\mathcal{L} = i\sqrt{2}e[(\bar{\psi}_L s_e + \bar{\psi}_R t_e)\tilde{\gamma} + \text{h.c.}], \quad (1)$$

where $\tilde{\gamma}$ is a Majorana spinor representing the photino. In the following we neglect the photino mass as well as the electron mass.

There are eight Feynman diagrams for the process $e^+e^- \rightarrow e^+\tilde{\gamma}t_e^-$, which are shown in fig. 1. When the mass of the scalar electron is lighter than the beam energy, scalar electron pair-production takes place and diagrams (4) and (5) are the dominant diagrams. While in case the mass is heavier than the beam energy, if the final e^+ is not observed and the integral over the e^+ variables is performed in the entire kinematically allowed region, the one-photon exchange diagrams (1) and (2) dominate over the other diagrams. For this reason, only these two diagrams are considered in ref. [5]. In the present case, however, we want to detect the e^+ in the final state. This specially means that we must exclude the very forward direction from the integral over the e^+ variables, since due to experimental conditions, one cannot detect

the final e^+ which is scattered in the very forward direction. Then the contribution from the other diagrams is not negligible. We have to take all these diagrams into consideration, although we can expect that, depending on the beam energy or the kinematical region we are interested in, some of the diagrams are suppressed.

Note that in diagrams (7) and (8), the photino propagator does not conserve fermion number, characteristic to Majorana particles. In addition to the photino, the goldstino, the goldstone fermion also couples to leptons and the corresponding scalar leptons with a similar lagrangian as (1). However, when gravity is introduced in the theory, the goldstino is eaten by the generalized Higgs mechanism and the gravitino \tilde{G} acquires a mass [7]. For this reason we do not consider the goldstino contribution in diagrams (5) and (6).

The corresponding matrix elements for each diagram are expressed as follows. (The momenta of the particles are labeled in fig. 1)

$$\mathcal{M}^{(1)} = e^2 g [\bar{v}(p_1)\gamma_\mu v(p_2)] q^{-2}$$

$$\times [\bar{u}(k_3)\frac{1}{2}(1 + \gamma_5)(\not{q} + \not{k}_1)^{-1}\gamma^\mu u(k_1)],$$

$$\mathcal{M}^{(2)} = e^2 g [\bar{v}(p_1)\gamma_\mu v(p_2)] q^{-2}$$

$$\times \{\bar{u}(k_3)\frac{1}{2}(1 + \gamma_5)$$

$$\times \{(2k_4 - q)^\mu / [(k_4 - q)^2 - m_{t_e}^2]\} u(k_1)\},$$

$$\mathcal{M}^{(3)} = -e^2 g [\bar{v}(p_1)\gamma_\mu u(k_1)] \frac{1}{4} E_{\text{beam}}^{-2}$$

$$\times [\bar{u}(k_3)\frac{1}{2}(1 + \gamma_5)(\not{k}_3 + \not{k}_4)^{-1}\gamma^\mu v(p_2)],$$

$$\mathcal{M}^{(4)} = e^2 g [\bar{v}(p_1)\gamma_\mu u(k_1)] \frac{1}{4} E_{\text{beam}}^{-2}$$

$$\times \{\bar{u}(k_3)\frac{1}{2}(1 + \gamma_5)$$

$$\times \{(p_2 + k_3 - k_4)^\mu / [(p_2 + k_3)^2 - m_{t_e}^2]\} v(p_2)\},$$

$$\mathcal{M}^{(5)} = g^3 [\bar{v}(p_1)(\not{k}_1 - \not{k}_4)^{-1}\frac{1}{2}(1 + \gamma_5)u(k_1)]$$

$$\times [(k_3 + p_2)^2 - m_{t_e}^2]^{-1} [\bar{u}(k_3)\frac{1}{2}(1 + \gamma_5)v(p_2)],$$

$$\mathcal{M}^{(6)} = -g^3 [\bar{v}(p_1)(\not{k}_4 + \not{p}_2)^{-1}\frac{1}{2}(1 + \gamma_5)v(p_2)]$$

$$\times [(k_3 - k_1)^2 - m_{t_e}^2]^{-1} [\bar{u}(k_3)\frac{1}{2}(1 + \gamma_5)u(k_1)], \quad (2)$$

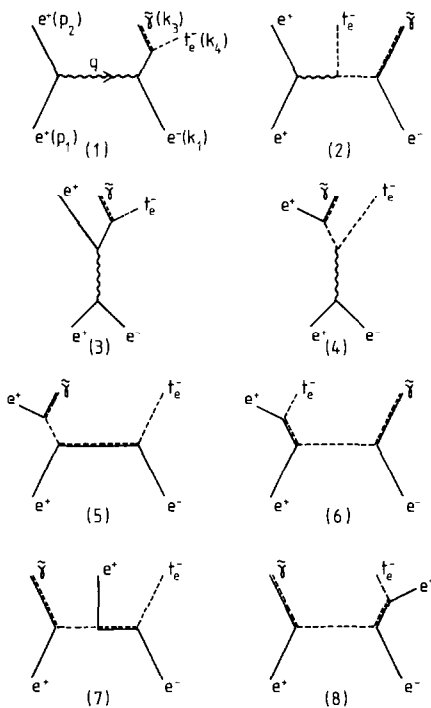


Fig. 1. Feynman diagrams for $e^+e^- \rightarrow e^+\tilde{\gamma}t_e^-$.

$$\begin{aligned} \mathcal{M}^{(7)} &= g^3 \{v(p_2)^T \frac{1}{2}(1 + \gamma_5) [-\gamma_0(\not{k}_1 - \not{k}_4)^{-1}] u(k_1)\} \\ &\quad \times [(p_1 - k_3)^2 - m_{s_e}^2]^{-1} [\bar{v}(p_1) \frac{1}{2}(1 + \gamma_5) v(k_3)], \\ \mathcal{M}^{(8)} &= g^3 \{v(p_2)^T \frac{1}{2}(1 + \gamma_5) [-\gamma_0(\not{k}_2 + \not{k}_4)^{-1}] u(k_1)\} \\ &\quad \times [(p_1 - k_3)^2 - m_{s_e}^2]^{-1} [\bar{v}(p_1) \frac{1}{2}(1 + \gamma_5) v(k_3)], \end{aligned} \quad (2 \text{ cont'd})$$

where $g = \sqrt{2}e$.

The matrix elements for the process $e^+e^- \rightarrow e^+\tilde{\gamma}s_e^-, e^+\tilde{\gamma}s_e^-$ are obtained from the above expression by replacing γ_5 with $-\gamma_5$ and interchanging m_{t_e} and m_{s_e} .

There are four independent variables, for which we take E' (scattered e^+ energy), ω (t_e energy), θ_e (e^+ scattering angle) and θ (t_e scattering angle). In terms of these variables the differential cross section is expressed as

$$\begin{aligned} d\sigma(e^+e^- \rightarrow e^+\tilde{\gamma}t_e^-)/dE' d\omega d\cos\theta_e d\cos\theta \\ = \frac{kE'}{16E_{\text{beam}}^2 (2\pi)^4} \frac{\sum'_{\text{spin}} |\sum_{i=1}^8 \mathcal{M}^{(i)}|^2}{(4E'^2 k^2 \sin^2\theta_e \sin^2\theta - \Psi^2)^{1/2}}, \end{aligned} \quad (3)$$

where

$$\begin{aligned} \Psi &= 4E_{\text{beam}}(E_{\text{beam}} - E' - \omega) + m_{t_e}^2 + 2E'\omega \\ &\quad - 2E'k \cos\theta \cos\theta_e \end{aligned}$$

and

$$k = (\omega^2 - m_{t_e}^2)^{1/2}.$$

The explicit calculation of the right-hand side is straightforward but tedious, the details of which will be given in a separate paper [8]. However, a couple of comments are in order. When $E_{\text{beam}} > m_{t_e}$, scalar electron pair production takes place and the diagrams (4) and (5) give rise to a divergence. We avoid this by introducing a total width to the scalar electron propagator with $\Gamma_{\text{tot}} = \Gamma(t_e \rightarrow e\tilde{\gamma}) = \alpha m_{t_e}/2$. The differential cross section for the process $e^+e^- \rightarrow e^+\tilde{\gamma}s_e^-$ is obtained from eq. (3) by interchanging m_{t_e} and m_{s_e} . In the following we assume that the two scalar electrons s_e and t_e have the same masses: $m_{s_e} = m_{t_e} \equiv m$, which is the case when their interactions with the photino preserve parity [9].

The result of the differential cross section $d\sigma/$

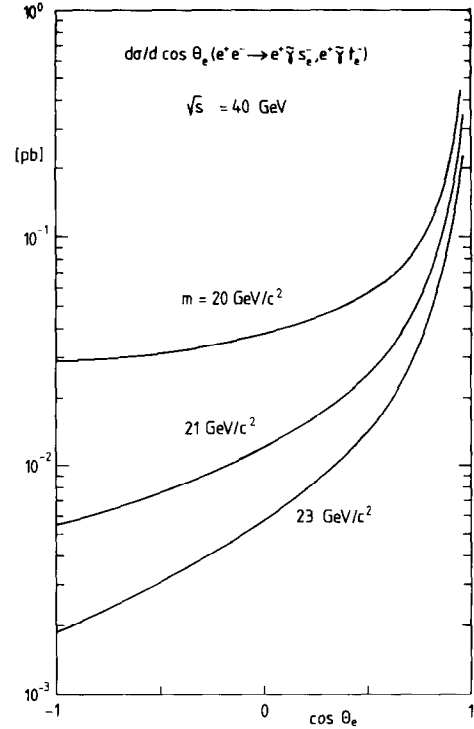


Fig. 2. The differential cross section $d\sigma(e^+e^- \rightarrow e^+\tilde{\gamma}s_e^-, e^+\tilde{\gamma}t_e^-)/d\cos\theta_e$ at $E_{\text{beam}} = 20$ GeV for several values of scalar electron mass.

$d\cos\theta_e$ at $E_{\text{beam}} = 20$ GeV is shown in fig. 2 for the various values of the scalar electron mass. A sharp peak at $\cos\theta_e = 1$ is seen, which comes from the diagrams (1) and (2). The total cross section at $E_{\text{beam}} = 20$ GeV versus m , the scalar electron mass, is plotted in fig. 3 for $|\cos\theta_e| < 0.8$ and without a cut on $\cos\theta_e$. The graph shows that if, for example, $m = 22$ GeV, the cross section for single scalar electron production is about 0.04 pb for $E_{\text{beam}} = 20$ GeV and the scalar electron will be easily detected at PETRA experiments. For example, with the integrated luminosity of 50 pb^{-1} , two events of scalar electron production are expected at the PETRA experiments.

For comparison, we included in fig. 3, the curve for the pair production of scalar electrons [3],

$$\begin{aligned} \sigma(e^+e^- \rightarrow t_e^+t_e^-; s_e^+s_e^-) &= (5\pi\alpha^2\beta^3/6E_{\text{beam}}^2) \\ &\quad \times \{1 + \frac{1}{2}\beta^2 + \frac{1}{4}\beta^4 + \frac{3}{20}[(5 + 2\beta^2 + \beta^1)/\beta^2]\} \\ &\quad \times \{\beta^{-1} \log[(1 + \beta)/(1 - \beta)] - 2 - \frac{2}{3}\beta^2\}, \end{aligned} \quad (4)$$

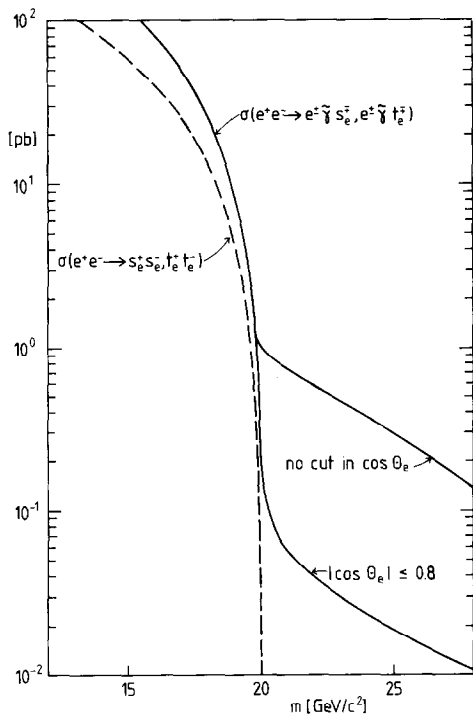


Fig. 3. The integrated cross section $\sigma(e^+e^- \rightarrow e^+\tilde{\gamma}s_e^\pm, e^+\tilde{\gamma}t_e^\pm)$ as a function of the scalar electron mass $m \equiv m_{t_e} = m_{s_e}$ at $E_{\text{beam}} = 20$ GeV. The dashed line represents the pair production cross section given in eq. (4).

where $\beta^2 = 1 - m^2/E_{\text{beam}}^2$. Since scalar electron pair production [diagrams (4) and (5) in fig. 1] dominates in the region $m < E_{\text{beam}}$, our curve coincides with the pair production curve when the former is divided by a factor 2. The factor 2 comes from the fact that in the pair production where both t_e^+ and t_e^- are on-shell, two cross sections $\sigma(e^+e^- \rightarrow t_e^+t_e^-; t_e^+ \rightarrow e^+\tilde{\gamma})$ and $\sigma(e^+e^- \rightarrow t_e^+t_e^-; t_e^- \rightarrow e^-\tilde{\gamma})$ originate from the same diagrams (4) and (5) and therefore there is a double counting in this region. The cross section $\sigma(e^+e^- \rightarrow e^+e^- + \text{missing energy})$, as is observed in actual experiments for the hunting of scalar electrons, is then given by $\sigma(e^+e^- \rightarrow t_e^+t_e^-, s_e^+s_e^-)$ for $m \lesssim E_{\text{beam}}$ and by $\sigma(e^+e^- \rightarrow e^+\tilde{\gamma}t_e^\pm, e^+\tilde{\gamma}s_e^\pm)$ for $m \gtrsim E_{\text{beam}}$ ^{‡3}.

In the region $m > E_{\text{beam}}$, our curve without cut for $\cos \theta_e$ coincides with the curve calculated in ref.

^{‡3} The explicit calculation of $\sigma(e^+e^- \rightarrow e^+e^- + \tilde{\gamma}\tilde{\gamma})$ with one of or both of $t_e^+(s_e^+)$ and $t_e^-(s_e^-)$ on-shell will be presented in ref. [8].

[5] using the Weizsäcker–Williams approximation.

In this paper we assumed the masses of the two scalar electrons t_e and s_e are the same. When the supersymmetry is spontaneously broken by the so-called F-term [10], it is expected [11] $m_{s_e} \gg m_{t_e}$. In this case, one searches for t_e in the process $e^+e^- \rightarrow e^+\tilde{\gamma}t_e^\pm$. Under the approximation of neglecting the electron mass, only the very massive s_e is exchanged in the propagators of the diagrams (7) and (8) of fig. 1, which makes the contribution from these diagrams very small, and the cross section in fig. 3 turns out to be enhanced by about 40% compared with the t_e production in the D-term symmetry breaking model.

Since the curve for pair production is very steeply falling near the threshold, it would be more practical to increase the beam energy in order to search for scalar electrons. When the energy is fixed and the mass of scalar electrons is higher than the beam energy, as it seems to be the case in the present PETRA experiments, then the process $e^+e^- \rightarrow e^+\tilde{\gamma}t_e^\pm (s_e^\pm)$ investigated in this paper, is one of the best and the cleanest processes to detect scalar electrons. Our estimate of the cross section indicates the necessity of high luminosity, which we expect to be achieved in PETRA experiments^{‡4}.

We would like to acknowledge T.F. Walsh for comments and discussions. M.K. thanks R. Baier for useful discussions. T.K. and S.Y. are grateful to Professor M. Koshiya for support. Those who were at DESY are indebted to the DESY directorate for their kind hospitality.

^{‡4} After completing the paper, the paper by Salati and Wallet (ref. [12]) came to our attention. They discuss the heavy gaugino ($\gtrsim 20$ GeV) production in the process $e^+e^- \rightarrow e + \text{gaugino} + \text{scalar electron}$ at LEP energy, in contrast to our case where the photino is light ($\lesssim 1$ GeV).

References

- [1] J. Wess and B. Zumino, Nucl. Phys. B70 (1974) 39; Phys. Lett. 49B (1974) 52; A. Salam and B. Strathdee, Phys. Rev. D11 (1975) 1521; P. Fayet and S. Ferrara, Phys. Rep. 32C (1977) 249.
- [2] For example, P. Fayet, talk XVIth Rencontre de Moriond (1981); C.H. Llewellyn Smith, talk CERN Supersymmetry workshop (1982), Oxford preprint, ref. 44/82.

- [3] G.R. Farrar and P. Fayet, Phys. Lett. 89B (1980) 191.
- [4] JADE Collab., W. Bartel et al., DESY 80/92 (1980);
CELLO Collab., H.J. Berhend et al., Phys. Lett. 114B (1982) 287;
TASSO Collab., R. Brandelik et al., Phys. Lett. 117B (1982) 365;
MARK J Collab., B. Adeva et al., Phys. Lett. 115B (1982) 345.
- [5] M.K. Gaillard, L. Hall and I. Hinchliffe, Phys. Lett. 116B (1982) 279.
- [6] J. Wess and B. Zumino, Nucl. Phys. B78 (1974) 1.
- [7] S. Deser and B. Zumino, Phys. Rev. Lett. 38 (1977) 1433.
- [8] T. Kobayashi and M. Kuroda, in preparation.
- [9] P. Fayet, Phys. Lett. 84B (1979) 416.
- [10] R. Barbieri, S. Ferrara and D.V. Nanopoulos, Phys. Lett. 116B (1982) 16.
- [11] L.E. Ibanez and G.G. Ross, Phys. Lett. 110B (1982) 215;
J. Ellis, L.E. Ibanez and G.G. Ross, Phys. Lett. 113B (1982) 283;
J. Ellis, J.S. Hagelin and D.V. Nanopoulos, Phys. Lett. 116B (1982) 283.
- [12] P. Salati and J.C. Wallet, Phys. Lett. 122B (1983) 397.